

See discussions, stats, and author profiles for this publication at: <https://www.researchgate.net/publication/6795702>

Microbial Fuel Cells: Methodology and Technology †

Article in *Environmental Science and Technology* · October 2006

DOI: 10.1021/es0605016 · Source: PubMed

CITATIONS

4,723

READS

19,817

9 authors, including:



Bruce E Logan

Pennsylvania State University

711 PUBLICATIONS 79,256 CITATIONS

[SEE PROFILE](#)



H.V.M. Hamelers

Wetsus

243 PUBLICATIONS 24,301 CITATIONS

[SEE PROFILE](#)



Uwe Schröder

University of Greifswald

226 PUBLICATIONS 17,659 CITATIONS

[SEE PROFILE](#)



Stefano Freguia

University of Melbourne

104 PUBLICATIONS 9,975 CITATIONS

[SEE PROFILE](#)

Some of the authors of this publication are also working on these related projects:



Bioelectrical fuel cell [View project](#)



Development of an optical sensor platform for in situ diagnostics of microbial fuel/electrolysis cells [View project](#)

Microbial Fuel Cells: Methodology and Technology[†]

BRUCE E. LOGAN,^{*,‡} BERT HAMELERS,[§]
RENÉ ROZENDAL,^{§,||} UWE SCHRÖDER,[⊥] JÜRG KELLER,[#]
STEFANO FREGUIA,[#] PETER AELTERMAN,[@]
WILLY VERSTRAETE,[@] AND KORNEEL RABAEY[@]

Hydrogen Energy Center, 212 Sackett Building, Penn State University, University Park, Pennsylvania, 16802, Sub-Department of Environmental Technology, Wageningen University, Bomenweg 2, P.O. Box 8129, 6700 EV Wageningen, The Netherlands, Wetsus, Centre for Sustainable Water Technology, Agora 1, P.O. Box 1113, 8900 CC Leeuwarden, The Netherlands, University of Greifswald, Institute of Chemistry and Biochemistry, Soldmannstrasse 16, 17489 Greifswald, Germany, Advanced Wastewater Management Centre (AWMC), The University of Queensland, St. Lucia, Brisbane, 4072 Australia, and Laboratory of Microbial Ecology and Technology (LabMET), Ghent University, Coupure Links 653, B-9000 Ghent, Belgium

Microbial fuel cell (MFC) research is a rapidly evolving field that lacks established terminology and methods for the analysis of system performance. This makes it difficult for researchers to compare devices on an equivalent basis. The construction and analysis of MFCs requires knowledge of different scientific and engineering fields, ranging from microbiology and electrochemistry to materials and environmental engineering. Describing MFC systems therefore involves an understanding of these different scientific and engineering principles. In this paper, we provide a review of the different materials and methods used to construct MFCs, techniques used to analyze system performance, and recommendations on what information to include in MFC studies and the most useful ways to present results.

Introduction

Microbial fuel cells (MFCs) are devices that use bacteria as the catalysts to oxidize organic and inorganic matter and generate current (1–5). Electrons produced by the bacteria from these substrates are transferred to the anode (negative terminal) and flow to the cathode (positive terminal) linked by a conductive material containing a resistor, or operated under a load (i.e., producing electricity that runs a device) (Figure 1). By convention, a positive current flows from the positive to the negative terminal, a direction opposite to that of electron flow. The device must be capable of having the substrate oxidized at the anode replenished, either continuously or intermittently; otherwise, the system is considered to be a biobattery. Electrons can be transferred to the anode by electron mediators or shuttles (6, 7), by direct membrane associated electron transfer (8), or by so-called nanowires (9–11) produced by the bacteria, or perhaps by other as yet undiscovered means. Chemical mediators, such as neutral

red or anthraquinone-2,6-disulfonate (AQDS), can be added to the system to allow electricity production by bacteria unable to otherwise use the electrode (12, 13). If no exogenous mediators are added to the system, the MFC is classified as a “mediator-less” MFC even though the mechanism of electron transfer may not be known (14).

In most MFCs the electrons that reach the cathode combine with protons that diffuse from the anode through a separator and oxygen provided from air; the resulting product is water (12, 15–17). Chemical oxidizers, such as ferricyanide or Mn (IV), can also be used although these must be replaced or regenerated (6, 18–20). In the case of metal ions, such as Mn that are reduced from Mn (IV) to Mn (II), bacteria can help to catalyze the reoxidation of the metal using dissolved oxygen (19, 20).

Microbially catalyzed electron liberation at the anode and subsequent electron consumption at the cathode, when both processes are sustainable, are the defining characteristics of an MFC. Using a sacrificial anode consisting of a slab of Mg alloy (20) does not, for example, qualify the system as an MFC as no bacteria are needed for catalyzing the oxidation of the fuel. Systems that use enzymes or catalysts not directly produced in situ by the bacteria in a sustainable manner are considered here as enzymatic biofuel cells and are well reviewed elsewhere (21).

MFCs operated using mixed cultures currently achieve substantially greater power densities than those with pure cultures (6, 7). In one recent test, however, an MFC showed high power generation using a pure culture, but the same device was not tested using acclimated mixed cultures and the cells were grown externally to the device (22). Community analysis of the microorganisms that exist in MFCs has so far revealed a great diversity in composition (6, 12, 23–25). We believe, based on existing data, and new data from our individual laboratories, that many new types of bacteria will be discovered that are capable of anodophilic electron transfer (electron transfer to an anode) or even interspecies electron transfer (electrons transferred between bacteria in any form).

MFCs are being constructed using a variety of materials, and in an ever increasing diversity of configurations. These systems are operated under a range of conditions that include differences in temperature, pH, electron acceptor, electrode surface areas, reactor size, and operation time. Potentials

* Corresponding author phone: 814-863-7908; fax: 814-863-7304; e-mail: blogan@psu.edu.

[†] This review is part of the Microbial Fuel Cells Focus Group.

[‡] Penn State University.

[§] Wageningen University.

^{||} Wetsus, Centre for Sustainable Water Technology.

[⊥] University of Greifswald.

[#] The University of Queensland.

[@] Ghent University.

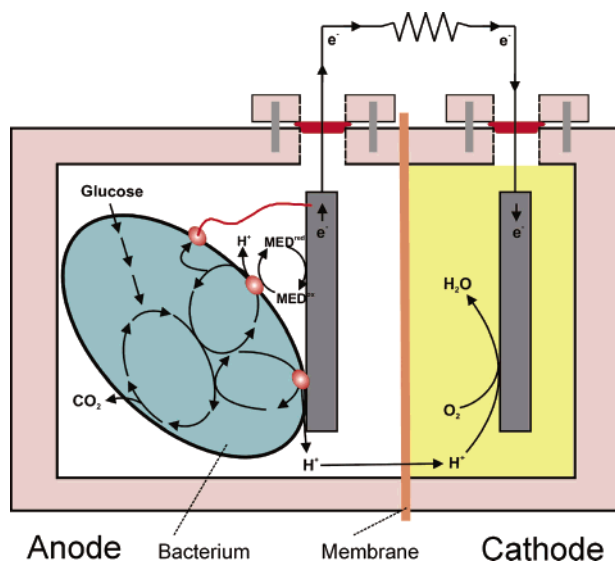


FIGURE 1. Operating principles of a MFC (not to scale). A bacterium in the anode compartment transfers electrons obtained from an electron donor (glucose) to the anode electrode. This occurs either through direct contact, nanowires, or mobile electron shuttles (small spheres represent the final membrane associated shuttle). During electron production protons are also produced in excess. These protons migrate through the cation exchange membrane (CEM) into the cathode chamber. The electrons flow from the anode through an external resistance (or load) to the cathode where they react with the final electron acceptor (oxygen) and protons (26).

are reported with different reference states, and sometimes only under a single load (resistor). The range of conditions, and in some cases a lack of important data like the internal resistance or power densities derived from polarization curves taken using different methods, has made it difficult to interpret and compare results among these systems (26). The variation in reported data has created a need to clarify methods of data collection and reporting. We have individually received many requests from researchers for details on construction of MFCs and for names of providers of materials

and equipment, indicating there is a need in the literature for a paper that provides a more comprehensive source of this information. In this paper, we therefore review existing types of MFCs, provide information on construction materials and give examples of manufacturers (although this should not be considered an endorsement of a particular company), and describe methods of data analysis and reporting in order to provide information to researchers interested in duplicating or advancing MFCs technologies. Additional information is available on the microbial fuel cell website (www.microbialfuelcell.org).

MFC Designs

Many different configurations are possible for MFCs (Figures 2 and 3). A widely used and inexpensive design is a two-chamber MFC built in a traditional “H” shape, consisting usually of two bottles connected by a tube containing a separator which is usually a cation exchange membrane (CEM) such as Nafion (12, 13, 23, 27) or Ultrex (18), or a plain salt bridge (27) (Figure 2a, f). The key to this design is to choose a membrane that allows protons to pass between the chambers (the CEM is also called a proton exchange membrane, PEM), but optimally not the substrate or electron acceptor in the cathode chamber (typically oxygen). In the H-configuration, the membrane is clamped in the middle of the tubes connecting the bottle (Figure 2f). However, the tube itself is not needed. As long as the two chambers are kept separated, they can be pressed up onto either side of the membrane and clamped together to form a large surface (Figure 2b). An inexpensive way to join the bottles is to use a glass tube that is heated and bent into a U-shape, filled with agar and salt (to serve the same function as a cation exchange membrane), and inserted through the lid of each bottle (Figure 2a). The salt bridge MFC, however, produces little power due the high internal resistance observed.

H-shape systems are acceptable for basic parameter research, such as examining power production using new materials, or types of microbial communities that arise during the degradation of specific compounds, but they typically produce low power densities. The amount of power that is generated in these systems is affected by the surface area of

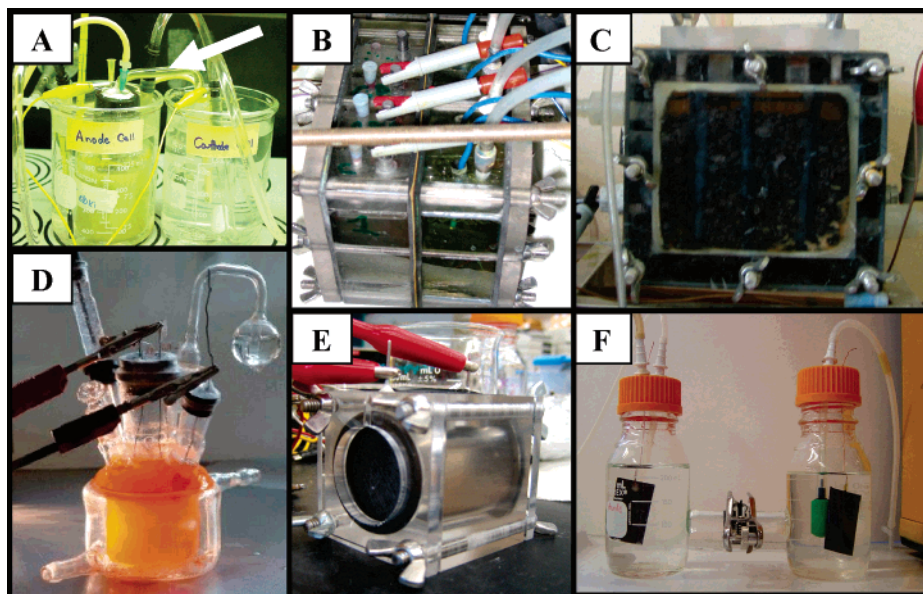


FIGURE 2. Types of MFCs used in studies: (A) easily constructed system containing a salt bridge (shown by arrow) (27); (B) four batch-type MFCs where the chambers are separated by the membrane (without a tube) and held together by bolts (7); (C) same as B but with a continuous flow-through anode (granular graphite matrix) and close anode–cathode placement (75); (D) photoheterotrophic type MFC (76); (E) single-chamber, air-cathode system in a simple “tube” arrangement (30); (F) two-chamber H-type system showing anode and cathode chambers equipped for gas sparging (23).

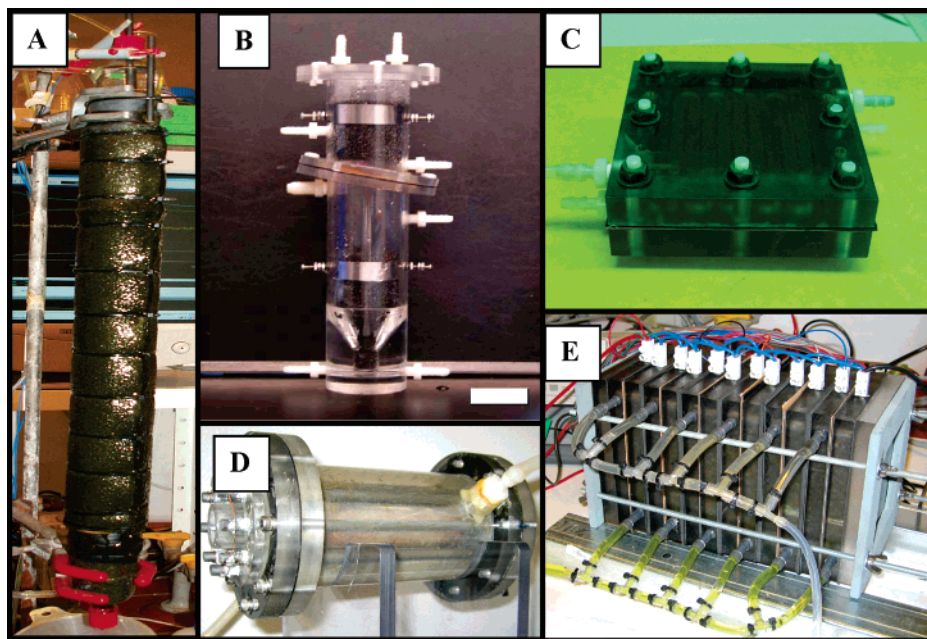


FIGURE 3. MFCs used for continuous operation: (A) upflow, tubular type MFC with inner graphite bed anode and outer cathode (35); (B) upflow, tubular type MFC with anode below and cathode above, the membrane is inclined (36); (C) flat plate design where a channel is cut in the blocks so that liquid can flow in a serpentine pattern across the electrode (17); (D) single-chamber system with an inner concentric air cathode surrounded by a chamber containing graphite rods as anode (34); (E) stacked MFC, in which 6 separate MFCs are joined in one reactor block (25).

the cathode relative to that of the anode (28) and the surface of the membrane (29). The power density (P) produced by these systems is typically limited by high internal resistance and electrode-based losses (see below). When comparing power produced by these systems, it makes the most sense to compare them on the basis of equally sized anodes, cathodes, and membranes (29).

Using ferricyanide as the electron acceptor in the cathode chamber increases the power density due to the availability of a good electron acceptor at high concentrations. Ferricyanide increased power by 1.5 to 1.8 times compared to a Pt-catalyst cathode and dissolved oxygen (H-design reactor with a Nafion CEM) (29). The highest power densities so far reported for MFC systems have been low internal resistance systems with ferricyanide at the cathode (6, 18). While ferricyanide is an excellent catholyte in terms of system performance, it must be chemically regenerated and its use is not sustainable in practice. Thus, the use of ferricyanide is restricted to fundamental laboratory studies.

It is not essential to place the cathode in water or in a separate chamber when using oxygen at the cathode. The cathode can be placed in direct contact with air (Figures 2e, 3c, 3d), either in the presence or absence of a membrane (30). In one system a kaolin clay-based separator and graphite cathode were joined to form a combined separator–cathode structure (31). Much larger power densities have been achieved using oxygen as the electron acceptor when aqueous-cathodes are replaced with air-cathodes. In the simplest configuration, the anode and cathode are placed on either side of a tube, with the anode sealed against a flat plate and the cathode exposed to air on one side, and water on the other (Figure 2e). When a membrane is used in this air-cathode system, it serves primarily to keep water from leaking through the cathode, although it also reduces oxygen diffusion into the anode chamber. The utilization of oxygen by bacteria in the anode chamber can result in a lower Coulombic efficiency (defined as the fraction of electrons recovered as current versus the maximum possible recovery; see below) (30). Hydrostatic pressure on the cathode will make it leak water, but that can be minimized by applying

coatings, such as polytetrafluoroethylene (PTFE), to the outside of the cathode that permit oxygen diffusion but limit bulk water loss (32).

Several variations on these basic designs have emerged in an effort to increase power density or provide for continuous flow through the anode chamber (in contrast to the above systems which were all operated in batch mode). Systems have been designed with an outer cylindrical reactor with a concentric inner tube that is the cathode (33, 34) (Figure 3d), and with an inner cylindrical reactor (anode consisting of granular media) with the cathode on the outside (35) (Figure 3a). Another variation is to design the system like an upflow fixed-bed biofilm reactor, with the fluid flowing continuously through porous anodes toward a membrane separating the anode from the cathode chamber (36) (Figure 3b). Systems have been designed to resemble hydrogen fuel cells, where a CEM is sandwiched between the anode and cathode (Figure 3c). To increase the overall system voltage, MFCs can be stacked with the systems shaped as a series of flat plates or linked together in series (25) (Figure 3e).

Sediment MFCs. By placing one electrode into a marine sediment rich in organic matter and sulfides, and the other in the overlying oxic water, electricity can be generated at sufficient levels to power some marine devices (37, 38). Protons conducted by the seawater can produce a power density of up to 28 mW/m². Graphite disks can be used for the electrodes (12, 37), although platinum mesh electrodes have also been used (38). “Bottle brush” cathodes used for seawater batteries may hold the most promise for long-term operation of unattended systems as these electrodes provide a high surface area and are made of noncorrosive materials (39). Sediments have also been placed into H-tube configured two-chamber systems to allow investigation of the bacterial community (12).

Modifications for Hydrogen Production. By “assisting” the potential generated by the bacteria at the anode with a small potential by an external power source (>0.25 V), it is possible to generate hydrogen at the cathode (40–43). These reactors, called bioelectrochemically assisted microbial reactors (BEAMRs) or biocatalyzed electrolysis systems, are not

true fuel cells, however, as they are operated to produce hydrogen, not electricity. Through modifications of the MFC designs described above (to contain a second chamber for capturing the hydrogen gas), it should be possible to develop many new systems for hydrogen production.

Materials of Construction

Anode. Anodic materials must be conductive, biocompatible, and chemically stable in the reactor solution. Metal anodes consisting of noncorrosive stainless steel mesh can be utilized (44), but copper is not useful due to the toxicity of even trace copper ions to bacteria. The most versatile electrode material is carbon, available as compact graphite plates, rods, or granules, as fibrous material (felt, cloth, paper, fibers, foam), and as glassy carbon. There are numerous carbon suppliers worldwide, for example E-TEK and Electrosynthesis Co. Inc. (USA), GEE Graphite Limited, Dewsbury (UK), Morgan, Grimbergen (Belgium), and Alfa-Aesar (Germany).

The simplest materials for anode electrodes are graphite plates or rods as they are relatively inexpensive, easy to handle, and have a defined surface area. Much larger surface areas are achieved with graphite felt electrodes (13, 45) which can have high surface areas ($0.47 \text{ m}^2\text{g}^{-1}$, GF series, GEE Graphite limited, Dewsbury, UK). However, not all the indicated surface area will necessarily be available to bacteria. Carbon fiber, paper, foam, and cloth (Toray) have been extensively used as electrodes. It has been shown that current increases with overall internal surface area in the order carbon felt > carbon foam > graphite (46). Substantially higher surface areas are achieved either by using a compact material like reticulated vitreous carbon (RVC; ERG Materials and Aerospace Corp., Oakland, CA) (36, 47) which is available with different pore sizes, or by using layers of packed carbon granules (Le Carbone, Grimbergen, Belgium) or beads (35, 48). In both cases maintaining high porosity is important to prevent clogging. The long term effect of biofilm growth or particles in the flow on any of the above surfaces has not been adequately examined.

To increase the anode performance, different chemical and physical strategies have been followed. Park et al. (31) incorporated Mn(IV) and Fe(III) and used covalently linked neutral red to mediate the electron transfer to the anode. Electrocatalytic materials such as polyanilins/Pt composites have also been shown to improve the current generation through assisting the direct oxidation of microbial metabolites (49–51).

Directing the water flow through the anode material can be used to increase power. Cheng et al. (52) found that flow directed through carbon cloth toward the anode, and decreasing electrode spacing from 2 to 1 cm, increased power densities (normalized to the cathode projected surface area) from 811 to 1540 mW/m² in an air-cathode MFC. The increase was thought to be due to restricted oxygen diffusion into the anode chamber, although the advective flow could have helped with proton transport toward the cathode as well. Increased power densities have been achieved using RVC in an upflow UASB type MFC (36) or in a granular anode reactor (35) with ferricyanide cathodes. Flow through an anode has also been used in reactors using exogenous mediators (48).

Cathode. Due to its good performance, ferricyanide ($\text{K}_3[\text{Fe}(\text{CN})_6]$) is very popular as an experimental electron acceptor in microbial fuel cells (31). The greatest advantage of ferricyanide is the low overpotential using a plain carbon cathode, resulting in a cathode working potential close to its open circuit potential. The greatest disadvantage, however, is the insufficient reoxidation by oxygen, which requires the catholyte to be regularly replaced (35). In addition, the long term performance of the system can be affected by diffusion of ferricyanide across the CEM and into the anode chamber.

Oxygen is the most suitable electron acceptor for an MFC due to its high oxidation potential, availability, low cost (it is free), sustainability, and the lack of a chemical waste product (water is formed as the only endproduct). The choice of the cathode material greatly affects performance, and is varied based on application. For sediment fuel cells, plain graphite disk electrodes immersed in the seawater above the sediment have been used (38). Due to the very slow kinetics of the oxygen reduction at plain carbon, and the resulting large overpotential, the use of such cathodes restricts the use of this noncatalyzed material to systems that can tolerate low performance. In seawater, oxygen reduction on carbon cathodes has been shown to be microbially supported (19, 20). Such microbially assisted reduction has also been observed for stainless steel cathodes which rapidly reduces oxygen when aided by a bacterial biofilm (53).

To increase the rate of oxygen reduction, Pt catalysts are usually used for dissolved oxygen (37) or open-air (gas diffusion) cathodes (34, 48). To decrease the costs for the MFC the Pt load can be kept as low as 0.1 mg cm^{-2} (54). The long term stability of Pt needs to be more fully investigated, and there remains a need for new types of inexpensive catalysts. Recently, noble-metal free catalysts that use pyrolyzed iron(II) phthalocyanine or CoTMPPP have been proposed as MFC cathodes (54, 55).

Membrane. The majority of MFC designs require the separation of the anode and the cathode compartments by a CEM. Exceptions are naturally separated systems such as sediment MFCs (37) or specially designed single-compartment MFCs (30, 32). The most commonly used CEM is Nafion (Dupont Co., USA), which is available from numerous suppliers (e.g., Aldrich and Ion Power, Inc.). Alternatives to Nafion, such as Ultrex CMI-7000 (Membranes International Incorp., Glen Rock, NJ) also are well suited for MFC applications (6) and are considerably more cost-effective than Nafion. When a CEM is used in an MFC, it is important to recognize that it may be permeable to chemicals such as oxygen, ferricyanide, other ions, or organic matter used as the substrate. The market for ion exchange membranes is constantly growing, and more systematic studies are necessary to evaluate the effect of the membrane on performance and long-term stability (56).

Fundamentals of Voltage Generation in MFCs

Thermodynamics and the Electromotive Force. Electricity is generated in an MFC only if the overall reaction is thermodynamically favorable. The reaction can be evaluated in terms of Gibbs free energy expressed in units of Joules (J), which is a measure of the maximal work that can be derived from the reaction (57, 58), calculated as

$$\Delta G_r = \Delta G_r^0 + RT \ln(\Pi) \quad (1)$$

where ΔG_r (J) is the Gibbs free energy for the specific conditions, ΔG_r^0 (J) is the Gibbs free energy under standard conditions usually defined as 298.15 K, 1 bar pressure, and 1 M concentration for all species, R ($8.31447 \text{ J mol}^{-1} \text{ K}^{-1}$) is the universal gas constant, T (K) is the absolute temperature, and Π (unitless) is the reaction quotient calculated as the activities of the products divided by those of the reactants. The standard reaction Gibbs free energy is calculated from tabulated energies of formation for organic compounds in water, available from many sources (59–61).

For MFC calculations, it is more convenient to evaluate the reaction in terms of the overall cell electromotive force (emf), E_{emf} (V), defined as the potential difference between the cathode and anode. This is related to the work, W (J), produced by the cell, or

$$W = E_{\text{emf}} Q = -\Delta G_r \quad (2)$$

TABLE 1. Standard Potentials E_0 and Theoretical Potentials for Typical Conditions in MFCs E_{MFC} (E_{MFC} Was Calculated Using Eq 5 and Half Cell Values from Ref 57; All Potentials Are Shown against NHE)

electrode	reaction	E_0 (V)	conditions	E_{MFC} (V)
anode	$2 \text{HCO}_3^- + 9 \text{H}^+ + 8 \text{e}^- \rightarrow \text{CH}_3\text{COO}^- + 4 \text{H}_2\text{O}$	0.187 ^a	$\text{HCO}_3^- = 5 \text{ mM}, \text{CH}_3\text{COO}^- = 5 \text{ mM}, \text{pH} = 7$	-0.296 ^b
cathode	$\text{O}_2 + 4 \text{H}^+ + 4 \text{e}^- \rightarrow 2 \text{H}_2\text{O}$	1.229	$\text{pO}_2 = 0.2, \text{pH} = 7$	0.805 ^b
	$\text{O}_2 + 4 \text{H}^+ + 4 \text{e}^- \rightarrow 2 \text{H}_2\text{O}$	1.229	$\text{pO}_2 = 0.2, \text{pH} = 10$	0.627
	$\text{MnO}_2(\text{s}) + 4 \text{H}^+ + 2 \text{e}^- \rightarrow \text{Mn}^{2+} + 2 \text{H}_2\text{O}$	1.23	$[\text{Mn}^{2+}] = 5 \text{ mM}, \text{pH} = 7$	0.470
	$\text{O}_2 + 2 \text{H}^+ + 2 \text{e}^- \rightarrow \text{H}_2\text{O}_2$	0.695	$\text{pO}_2 = 0.2, [\text{H}_2\text{O}_2] = 5 \text{ mM}, \text{pH} = 7$	0.328
	$\text{Fe}(\text{CN})_6^{3-} + \text{e}^- \rightarrow \text{Fe}(\text{CN})_6^{4-}$	0.361	$[\text{Fe}(\text{CN})_6^{3-}] = [\text{Fe}(\text{CN})_6^{4-}]$	0.361

^a Calculated from Gibbs free energy data tabulated in ref 61. ^b Note that an MFC with an acetate oxidizing anode ($\text{HCO}_3^- = 5 \text{ mM}, \text{CH}_3\text{COO}^- = 5 \text{ mM}, \text{pH} = 7$) and an oxygen reducing cathode ($\text{pO}_2 = 0.2, \text{pH} = 7$) has a cell emf of $0.805 - 0.296 = 1.101 \text{ V}$.

where $Q = nF$ is the charge transferred in the reaction, expressed in Coulomb (C), which is determined by the number of electrons exchanged in the reaction, n is the number of electrons per reaction mol, and F is Faraday's constant ($9.64853 \times 10^4 \text{ C/mol}$). Combining these two equations, we have

$$E_{\text{emf}} = -\frac{\Delta G_r}{nF} \quad (3)$$

If all reactions are evaluated at standard conditions, $\Pi = 1$, then

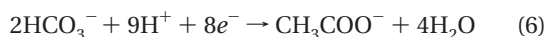
$$E_{\text{emf}}^0 = -\frac{\Delta G_r^0}{nF} \quad (4)$$

where E_{emf}^0 (V) is the standard cell electromotive force. We can therefore use the above equations to express the overall reaction in terms of the potentials as

$$E_{\text{emf}} = E_{\text{emf}}^0 - \frac{RT}{nF} \ln(\Pi) \quad (5)$$

The advantage of eq 5 is that it is positive for a favorable reaction, and directly produces a value of the emf for the reaction. This calculated emf provides an upper limit for the cell voltage; the actual potential derived from the MFC will be lower due to various potential losses (see below).

Standard Electrode Potentials. The reactions occurring in the MFC can be analyzed in terms of the half cell reactions, or the separate reactions occurring at the anode and the cathode. According to the IUPAC convention, standard potentials (at 298 K, 1 bar, 1 M) are reported as a reduction potential, i.e., the reaction is written as consuming electrons (57). For example, if acetate is oxidized by bacteria at the anode we write the reaction as

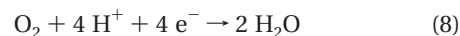


The standard potentials are reported relative to the normal hydrogen electrode (NHE), which has a potential of zero at standard conditions (298 K, $\text{pH}_2 = 1 \text{ bar}, [\text{H}^+] = 1 \text{ M}$). To obtain the theoretical anode potential, E_{An} , under specific conditions, we use eq 5, with the activities of the different species assumed to be equal to their concentrations. For acetate oxidation (Table 1), we therefore have

$$E_{\text{An}} = E_{\text{An}}^0 - \frac{RT}{8F} \ln \left(\frac{[\text{CH}_3\text{COO}^-]}{[\text{HCO}_3^-]^2 [\text{H}^+]^9} \right) \quad (7)$$

For the theoretical cathode potential, E_{cat} , if we consider the case where oxygen is used as the electron acceptor for

the reaction, we can write



$$E_{\text{cat}} = E_{\text{cat}}^0 - \frac{RT}{4F} \ln \left(\frac{1}{\text{pO}_2 [\text{H}^+]^4} \right) \quad (9)$$

A variety of catholytes has been used, and for each of these the cell voltage varies. For example, manganese oxide and ferricyanide have been used as alternatives to oxygen. The pH of the cathode solution can also vary, affecting the overall cathode potential. Using eq 9 and tabulated standard potentials available for inorganic compounds (57) for several different conditions, it can be seen that the theoretical cathode potential for these different catholytes range from 0.361 to 0.805 V.

The cell emf is calculated as

$$E_{\text{emf}} = E_{\text{cat}} - E_{\text{an}} \quad (10)$$

where the minus sign is a result of the definition of the anode potential as reduction reaction (although an oxidation reaction is occurring). Note that the result using eq 10 equals that of eq 3 and eq 5 only if the pH at the anode and the cathode are equal. Equation 10 demonstrates that using the same anode in a system with different cathode conditions as listed in Table 1 would produce significantly different cell voltages, and thus different levels of power output. The power produced by an MFC therefore depends on the choice of the cathode, and this should be taken into account when comparing power densities achieved by different MFCs.

Open Circuit Voltage (OCV). The cell emf is a thermodynamic value that does not take into account internal losses. The open circuit voltage (OCV) is the cell voltage that can be measured after some time in the absence of current. Theoretically, the OCV should approach the cell emf. In practice, however, the OCV is substantially lower than the cell emf, due to various potential losses. For example, a typical measured potential of a cathode using oxygen at pH 7 is about 0.2 V. This is clearly lower than the expected value of 0.805 V, indicating the large energy loss occurring at the cathode. This energy loss is often referred to as overpotential, or the difference between the potential under equilibrium conditions and the actual potential, which for this case is 0.605 V ($0.805 \text{ V} - 0.2 \text{ V}$). This illustrates that the main application of thermodynamic calculations is to identify the size and nature of energy losses.

Identifying Factors that Decrease Cell Voltage

The maximum attainable MFC voltage (emf) is theoretically on the order of 1.1 V (see above). However, the measured MFC voltage is considerably lower due to a number of losses. In an open circuit, when no current is flowing, the maximum MFC voltage achieved thus far is 0.80 V (62). During current generation, voltages achieved up to now remain below 0.62

V (35). In general, the difference between the measured cell voltage and the cell emf is referred to as overvoltage and is the sum of the overpotentials of the anode and the cathode, and the ohmic loss of the system

$$E_{cell} = E_{emf} - (\Sigma\eta_a + |\Sigma\eta_c| + IR_{\Omega}) \quad (11)$$

where $\Sigma\eta_a$ and $|\Sigma\eta_c|$ are the overpotentials of the anode and the cathode respectively, and IR_{Ω} is the sum of all ohmic losses which are proportional to the generated current (I) and ohmic resistance of the system (R_{Ω}). The overpotentials of the electrodes are generally current dependent and in an MFC they can roughly be categorized as follows: (i) activation losses; (ii) bacterial metabolic losses; and (iii) mass transport or concentration losses (see below).

In MFCs the measured cell voltage is usually a linear function of the current (see discussion of the polarization curve below), and can be described simply as

$$E_{cell} = OCV - IR_{int} \quad (12)$$

where IR_{int} is the sum of all internal losses of the MFC, which are proportional to the generated current (I) and internal resistance of the system (R_{int}). A comparison of eqs 11 and 12 shows that the overpotentials of the anode and the cathode that occur under open circuit conditions are included in the value of OCV in eq 12, while the current dependent overpotentials of the electrodes and ohmic losses of the system are captured in IR_{int} . MFC systems that are well described by eq 12 show a maximum power output when the internal resistance, R_{int} , is equal to external resistance, R_{ext} (52). Although R_{int} includes more than just ohmic resistance (R_{Ω}), both terms are often used interchangeably but MFC researchers should be aware of the differences in these two terms. MFC performance can be assessed in terms of both overpotentials and ohmic losses or in terms of OCV and internal losses, based on various techniques discussed below.

Ohmic Losses. The ohmic losses (or ohmic polarization) in an MFC include both the resistance to the flow of electrons through the electrodes and interconnections, and the resistance to the flow of ions through the CEM (if present) and the anodic and cathodic electrolytes (63, 64). Ohmic losses can be reduced by minimizing the electrode spacing, using a membrane with a low resistivity, checking thoroughly all contacts, and (if practical) increasing solution conductivity to the maximum tolerated by the bacteria.

Activation Losses. Due to the activation energy needed for an oxidation/reduction reaction, activation losses (or activation polarization) occur during the transfer of electrons from or to a compound reacting at the electrode surface. This compound can be present at the bacterial surface, as a mediator in the solution (Figure 4), or as the final electron acceptor reacting at the cathode. Activation losses often show a strong increase at low currents and steadily increase when current density increases. Low activation losses can be achieved by increasing the electrode surface area, improving electrode catalysis, increasing the operating temperature, and through the establishment of an enriched biofilm on the electrode(s).

Bacterial Metabolic Losses. To generate metabolic energy, bacteria transport electrons from a substrate at a low potential (e.g., Table 1: acetate -0.296 V) through the electron transport chain to the final electron acceptor (such as oxygen or nitrate) at a higher potential. In an MFC, the anode is the final electron acceptor and its potential determines the energy gain for the bacteria. The higher the difference between the redox potential of the substrate and the anode potential, the higher the possible metabolic energy gain for the bacteria, but the lower the maximum attainable MFC voltage. To

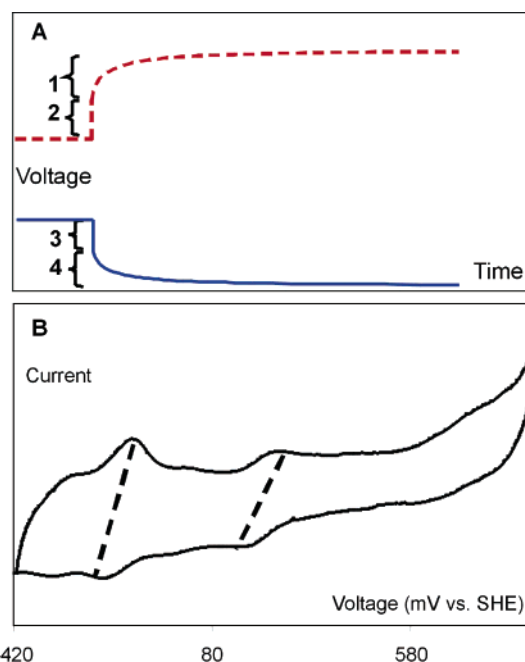


FIGURE 4. Electrochemical analysis of microbial fuel cells. (A) Anodic (blue solid line) and cathodic (red dashed line) voltage profiles over time when applying the current interrupt method for determination of the ohmic resistance of an MFC. Sections 2 and 3 indicate the voltage differences related to the ohmic resistance; sections 1 and 4 indicate voltage losses caused by the activation overpotentials. (B) Cyclic voltammogram (solid line) of an electrochemically active mixed microbial community. The dashed lines connect the oxidation and reduction peaks of redox active compounds (6).

maximize the MFC voltage, therefore, the potential of the anode should be kept as low (negative) as possible. However, if the anode potential becomes too low, electron transport will be inhibited and fermentation of the substrate (if possible) may provide greater energy for the microorganisms. The impact of a low anode potential, and its possible impact on the stability of power generation, should be addressed in future studies.

Concentration Losses. Concentration losses (or concentration polarization) occur when the rate of mass transport of a species to or from the electrode limits current production (63, 64). Concentration losses occur mainly at high current densities due to limited mass transfer of chemical species by diffusion to the electrode surface. At the anode concentration losses are caused by either a limited discharge of oxidized species from the electrode surface or a limited supply of reduced species toward the electrode. This increases the ratio between the oxidized and the reduced species at the electrode surface which can produce an increase in the electrode potential. At the cathode side the reverse may occur, causing a drop in cathode potential. In poorly mixed systems diffusional gradients may also arise in the bulk liquid. Mass transport limitations in the bulk fluid can limit the substrate flux to the biofilm, which is a separate type of concentration loss. By recording polarization curves, the onset of concentration losses can be determined as described below.

Instruments for Measurement

In addition to conventional instruments used for chemical measurements in microbial systems (e.g., for determining substrate concentrations and degradation products), MFC experiments can require specialized electrochemical instrumentation (6, 30). In most cases, cell voltages and electrode potentials are adequately measured with commonly available

voltage meters, multimeters, and data acquisition systems connected in parallel with the circuit. Cell voltages can be determined directly from the voltage difference between the anode and cathode; electrode potentials can only be determined against a reference electrode that needs to be included in the electrode compartment (65). Current is calculated using Ohm's law ($I = E_{cell}/R$) using the measured voltage.

A more detailed understanding of the (bio-)electrochemical system can be obtained using a potentiostat (e.g., Ecochemie, The Netherlands; Princeton Applied Research, USA; Gamry Scientific, USA). With a potentiostat either the potential or the current of an electrode can be controlled in order to study the electrochemical response of the electrode at that specific condition. The potentiostat is typically operated in a three-electrode-setup consisting of a working electrode (anode or cathode), a reference electrode, and a counter electrode (65). In MFC experiments, the potentiostatic mode of this instrument is often used for voltammetry tests in which the potential of the working electrode (anode or cathode) is varied at a certain scan rate (expressed in $V s^{-1}$). In the case where a scan only goes in one direction the method is referred to as linear sweep voltammetry (LSV); if the scan is also continued in the reverse direction and comes back to the start potential the method is cyclic voltammetry (CV; Figure 4B). Voltammetry can be used for assessing the electrochemical activity of microbial strains or consortia (6, 16, 50, 51), determining the standard redox potentials of redox active components (7), and testing the performance of novel cathode materials (55). A potentiostat can also be operated in a two-electrode setup to obtain polarization curves or to determine the ohmic resistance using the current interrupt technique (Figure 4A) as described below. In the two-electrode setup, the working electrode connector is connected to the cathode (positive terminal) and both the counter electrode and reference electrode connectors are connected to the anode.

More advanced measurements can be done when the potentiostat is equipped with a frequency response analyzer (FRA), allowing electrochemical impedance spectroscopy measurements (EIS) (65). In EIS a sinusoidal signal with small amplitude is superimposed on the applied potential of the working electrode. By varying the frequency of the sinusoidal signal over a wide range (typically 10^{-4} to 10^6 Hz) and plotting the measured electrode impedance, detailed information can be obtained about the electrochemical system. EIS can be used to measure the ohmic and internal resistance of an MFC (27, 66), as well as to provide additional insight into the operation of an MFC. The interpretation of EIS data can be rather complex, however, and therefore EIS techniques will not be discussed further here.

Calculations and Procedures for Reporting Data

Electrode Potential. The potential of an electrode (anode or cathode) can only be determined by measuring the voltage against an electrode with a known potential, i.e., a reference electrode. A reference electrode consists of several phases of constant composition (65) and therefore has a constant potential. The standard hydrogen electrode (SHE) or normal hydrogen electrode (NHE), consisting of a platinum electrode in a hydrogen saturated acidic solution (all components at unit activity), has a potential of 0 V. Because the NHE is not a very practical reference electrode to work with in an experimental setup, other reference electrodes are often used. The most popular reference electrode in MFC experiments is the silver–silver chloride (Ag/AgCl) reference electrode, because of its simplicity, stability, and nontoxicity. In a saturated potassium chloride solution at 25 °C the Ag/AgCl reference electrode develops a potential of +0.197 V against the NHE. Also practical, but less common in MFC experiments, is the saturated calomel electrode (SCE, 0.242 V against

the NHE). Electrode potentials are often strongly dependent on the pH in the system and it is therefore important to report the solution pH. Preferably, electrode potentials are reported in the literature back-calculated against the NHE (expressed in V or V vs NHE), but are also often reported as a voltage difference against the reference electrode that was used in the study (e.g., V vs Ag/AgCl).

As a consequence of these different methods, the potential of the electrodes appears to vary dependent on the electrode used, the pH, and for the cathode the concentration of the electron acceptor. For example, at pH 7 a typical anode potential is −0.20 to −0.28 V (NHE), equivalent to −0.40 to −0.48 V vs Ag/AgCl. At the same pH a typical cathode potential is 0.30 to 0.10 V (NHE), equivalent to 0.10 to −0.10 V vs Ag/AgCl.

Power. The overall performance of an MFC is evaluated in many ways, but principally through power output and Coulombic efficiency. Power is calculated as

$$P = IE_{cell} \quad (13)$$

Normally the voltage is measured across a fixed external resistor (R_{ext}), while the current is calculated from Ohm's law ($I = E_{cell}/R_{ext}$). Thus, power is usually calculated as

$$P = \frac{E_{cell}^2}{R_{ext}} \quad (14)$$

This is the direct measure of the electric power. The maximum power is calculated from the polarization curve (see below).

Power Density. Power is often normalized to some characteristic of the reactor in order to make it possible to compare power output of different systems. The choice of the parameter that is used for normalization depends on application, as many systems are not optimized for power production. The power output is usually normalized to the projected anode surface area because the anode is where the biological reaction occurs (6, 31, 34, 67). The power density (P_{An} , W/m^2) is therefore calculated on the basis of the area of the anode (A_{An}) as

$$P_{An} = \frac{E_{cell}^2}{A_{An}R_{ext}} \quad (15)$$

In many instances, however, the cathode reaction is thought to limit overall power generation (30, 32) or the anode consists of a material which can be difficult to express in terms of surface area (i.e., granular material; (35)). In such cases the area of the cathode (A_{Cat}) can alternatively be used to obtain a power density (P_{Cat}). The projected surface areas of all components should always be clearly stated, as well as the specific surface area (if known) and the method of its determination.

To perform engineering calculations for size and costing of reactors, and as a useful comparison to chemical fuel cells, the power is normalized to the reactor volume, or

$$P_v = \frac{E_{cell}^2}{\nu R_{ext}} \quad (16)$$

where P_v is the volumetric power (W/m^3) (68), and ν is the total reactor volume (i.e., the empty bed volume). The use of the total bed reactor volume is consistent with a tradition in environmental engineering to use the total reactor size as a basis for the calculation. A comparison on the basis of total reactor volume, however, is not always level when comparing two- and single-chambered reactors because there is no "second chamber" for an open air cathode. In such cases it is useful to compare reactors on the basis of the total anode

compartment volume. If multiple reactors are operated in concert, for example as a series of stacked reactors, the volume used for the air-space for the cathode (or volume for the catholyte) is then included for the overall reactor volume. Thus, the volume used in the calculation should be clearly stated, and volumes of the individual chambers must always be clearly noted.

Ohmic Resistance Using the Current Interrupt Technique. The ohmic resistance (R_Ω) of an MFC can be determined using the current interrupt technique (63, 64) by operating the MFC at a current at which no concentration losses occur. Next the electrical circuit is opened (which results in zero current, i.e., an infinite resistance) and a steep initial potential rise (E_R , Figure 4A voltage differences 2 + 3) is observed, followed by a slower further increase of the potential (E_A , Figure 4A voltage differences 1 + 4) to the OCV. The determination of the steep potential rise after current interrupting requires the fastest possible recording of the potential (up to μs scale) (64). Ohmic losses (IR_Ω) are proportional to the produced current and the ohmic resistance. When the current is interrupted the ohmic losses instantaneously disappear. This results in a steep potential rise (E_R) in potential that is proportional to the ohmic resistance (R_Ω) and the current (I) produced before the interruption (Figure 4A; see sections 2 and 3). Using Ohm's law, R_Ω is estimated using this approach as $R_\Omega = E_R/I$. The slower further increase of the potential (E_A) to the OCV after the initial steep potential rise gives the electrode overpotentials that occurred during current generation.

Polarization Curves. Polarization curves represent a powerful tool for the analysis and characterization of fuel cells (63). A polarization curve represents the voltage as a function of the current (density). Polarization curves can be recorded for the anode, the cathode, or for the whole MFC using a potentiostat. If a potentiostat is not available, a variable resistor box can be used to set variable external loads. Using a periodical decrease (or increase, when starting at short circuit) of the load, the voltage is measured and the current is calculated using Ohm's law. To separately study the performance of the system in terms of anode or cathode potentials, a reference electrode is used as described above. When a potentiostat is used to record a polarization curve, an appropriate scan rate should be chosen such as 1 mV s^{-1} (25). The polarization curve should be recorded both up and down (i.e., from high to low external resistance) and vice versa. When a variable external resistance is used to obtain a polarization curve, the current and potential values need to be taken only when pseudo-steady-state conditions have been established. The establishment of this pseudo-steady state may take several minutes or more, depending on the system and the external resistance. This condition is only a temporary steady state because over longer times the substrate concentration in the reactor will change due to substrate demand at the anode (unless continuously replenished). This will in turn affect the incidence of substrate/products mass transfer over voltage and current. Care should therefore be taken not to wait too long for the establishment of the pseudo-steady state. Polarization curves can also be obtained over multiple batch cycles, i.e., with one resistor used for the whole cycle, allowing measurement of Coulombic efficiency (see below) for each resistor (see ref 69 for a comparison of these two methods). Long-term recording may risk shifts in the microbial community.

Polarization curves can generally be divided in three zones: (i) starting from the OCV at zero current, there is an initial steep decrease of the voltage: in this zone the activation losses are dominant; (ii) the voltage then falls more slowly and the voltage drop is fairly linear with current: in this zone the ohmic losses are dominant; (iii) there is a rapid fall of the voltage at higher currents: in this zone the concentration

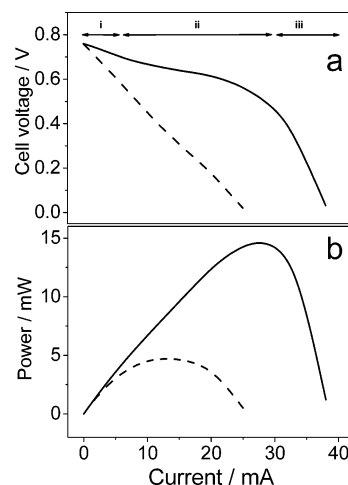


FIGURE 5. Polarization (a) and power (b) curves of a microbial fuel cell operating on starch. The solid curves are the original data (70), the dashed curves represent a mathematically manipulated dataset in which the effect of an increase of the ohmic resistance with 20Ω is illustrated. The increase of the ohmic resistance resulted in a linear polarization curve (dashed line). From the slope of this curve an internal resistance of 30 ohm can be determined.

losses (mass transport effects) are dominant (solid line, Figure 5A). In MFCs, linear polarization curves are most often encountered (dashed line, Figure 5A). For a linear polarization curve, the value of the internal resistance (R_{int}) of the MFC is easily obtained from the polarization curve as it is equal to the slope (e.g., $R_{int} = -\Delta E/\Delta I = 26 \Omega$; Figure 5A, dashed line).

Power Curves. A power curve that describes the power (or power density) as the function of the current (or current density) is calculated from the polarization curve. Figure 5B (solid line) shows a typical power curve based on a previously reported polarization curve (Figure 5A; 70). As no current flows for open circuit conditions, no power is produced. From this point onward, the power increases with current to a maximum power point, MPP (14.6 mW, Figure 5B). Beyond this point, the power drops due to the increasing ohmic losses and electrode overpotentials to the point where no more power is produced (short circuit conditions).

In many MFCs the ohmic resistance plays a dominant role in defining the point of the maximum attainable power (MPP), partially due to the low ionic conductivity of the substrate solutions (71), but usually to a low degree of optimization in the fuel cell design. The effect of increased ohmic resistance on the shape of a polarization curve is shown in Figure 5A. The solid curve is the original data set, while the dashed curve was calculated by including an additional ohmic resistance of $\Delta R_\Omega = 20 \Omega$ by subtracting a potential drop of $\Delta E_{IR} = I \Delta R_\Omega$. Increasing the ohmic resistance by this amount produces a polarization curve that is linear (Figure 5A, dashed line), which is typically observed for MFCs. When a polarization curve is linear the slope is equal to the internal resistance (eq 12), which for this example is calculated as $R_{int} = 30 \Omega$ (dashed line). If the polarization curve is not linear (solid line), a current independent R_{int} cannot be defined and the system is better expressed in terms of ohmic resistance R_Ω and the electrode overpotentials $\Sigma \eta_a$ and $|\Sigma \eta_c|$ (eq 11), which can be determined using the current interrupt method or EIS. Increasing the ohmic resistance decreases the MPP from 14.6 to 4.8 mW. A symmetrical semi-cycle power density curve is typical for a high internal resistance MFC limited by ohmic resistance (dashed line, Figure 5B) rather than a fuel cell limited by mass transfer (solid line, Figure 5B). In the case of a symmetrical semi-cycle, the MPP will occur at a point where the $R_{int} = R_{ext}$.

Treatment Efficiency. MFCs have been proposed as a method to treat wastewater, and thus it is important to evaluate the overall performance in terms of biochemical oxygen demand (BOD), chemical oxygen demand (COD), or total organic carbon (TOC) removal. Other factors may also be important, such as soluble versus particulate removal, and nutrient removal. We focus here on performance in terms of COD removal as it is a common measure for wastewater treatment efficiency, and the COD removal is needed for Coulombic and energy calculations. The COD removal efficiency (ϵ_{COD}) can be calculated as the ratio between the removed and influent COD. This parameter measures how much of the available “fuel” has been converted in the MFC, either into electrical current (via the Coulombic efficiency) or biomass (via the growth yield) or through competitive reactions with alternative electron acceptors (e.g., oxygen, nitrate, and sulfate). As the MFC influent can contain both dissolved and particulate COD, it can be difficult to specify what fraction of the effluent particulate COD was due to biomass produced in the reactor, or untreated COD that was originally in the reactor influent.

Coulombic Efficiency. The Coulombic efficiency, ϵ_c , is defined as the ratio of total Coulombs actually transferred to the anode from the substrate, to maximum possible Coulombs if all substrate removal produced current. The total Coulombs obtained is determined by integrating the current over time, so that the Coulombic efficiency for an MFC run in fed-batch mode, ϵ_{cb} , evaluated over a period of time t_b , is calculated as (35, 52)

$$\epsilon_{\text{cb}} = \frac{M \int_0^{t_b} I dt}{F b v_{\text{An}} \Delta \text{COD}} \quad (17)$$

where $M = 32$, the molecular weight of oxygen, F is Faraday's constant, $b = 4$ is the number of electrons exchanged per mole of oxygen, v_{An} is the volume of liquid in the anode compartment, and ΔCOD is the change in COD over time t_b . For continuous flow through the system, we calculate the Coulombic efficiency, ϵ_{cb} , on the basis of current generated under steady conditions as

$$\epsilon_{\text{cb}} = \frac{MI}{F b q \Delta \text{COD}} \quad (18)$$

where q is the volumetric influent flow rate and ΔCOD is the difference in the influent and effluent COD.

The Coulombic efficiency is diminished by utilization of alternate electron acceptors by the bacteria, either those present in the medium (or wastewater), or those diffusing through the CEM such as oxygen. Other factors that reduce Coulombic efficiency are competitive processes and bacterial growth. Bacteria unable to utilize the electrode as electron acceptor are likely to use substrate for fermentation and/or methanogenesis. It has been observed that fermentative patterns diminish through time during enrichment of the microbial consortium in the MFC (6). As long as the anode remains attractive enough for the bacteria due to its potential, alternative electron acceptors will not be used. However, high potential compounds such as nitrate (+0.55 V) will almost certainly be used.

Growth Yield. Cell growth will reduce ϵ_c due to diversion of electrons into biomass. The substrate utilization for growth is measured by the net (or observed) cell yield, Y , calculated as

$$Y = \frac{X}{\Delta \text{COD}} \quad (19)$$

where X is the biomass (g COD) produced over time (either t_b or hydraulic retention time). An important advantage of

an MFC is the lower cell yield compared to aerobic processes. This is caused by the reduced energy available for biomass growth as a significant part of the substrate energy is converted to electrical power. Reported MFC net yields range from 0.07 and 0.22 g biomass COD (g substrate COD)⁻¹, while typical aerobic yields for wastewater treatment are generally around 0.4 g biomass COD (g substrate COD)⁻¹ (26). The growth rate can be measured directly by determining the biomass (g COD) built up on the electrode surface and discharged in the effluent (for continuous operation). The low biomass production in MFCs is an especially attractive benefit since sludge disposal by combustion (becoming the standard technology in Europe) costs approximately 600 Euros per tonne.

COD Balance. Once the efficiencies for electricity and biomass production are completed, the fraction of COD that was removed by unknown processes, φ , can be calculated as

$$\varphi = 1 - \epsilon_c - Y \quad (20)$$

Loading Rate. When examining the use of MFCs for wastewater treatment, it is useful to examine performance achieved with this new technology in terms of loading rates with those typically obtained in conventional treatment systems. To do this, we calculate the loading based on volumetric loading rates as B_v (kg COD m⁻³ d⁻¹). Typical values for B_v achieved to date are up to 3 kg COD m⁻³ d⁻¹ (18), compared to values for high-rate anaerobic digestion of 8–20 kg COD m⁻³ d⁻¹ or activated sludge processes of 0.5–2 kg COD m⁻³ d⁻¹. These loading rates can be normalized to the total anode volume for comparison with suspended biomass processes (e.g., activated sludge, anaerobic digestion), and to total anode surface area for comparison with biofilm processes. Based on the reported areal short-term peak power productions (3, 46), the anode surface-specific conversion rates for MFCs are up to 25–35 g COD m⁻² d⁻¹, which is higher than typical loading rates for rotating biological contactors (RBCs; 10–20 g COD m⁻² d⁻¹; 72) and comparable to those of high rate aerobic biofilm processes such as the moving bed bio-reactors (MBBRs).

Energy Efficiency. The most important factor for evaluating the performance of an MFC for making electricity, compared to more traditional techniques, is to evaluate the system in terms of the energy recovery. The overall energetic efficiency, ϵ_E , is calculated as the ratio of power produced by the cell over a time interval t to the heat of combustion of the organic substrate added in that time frame, or

$$\epsilon_E = \frac{\int_0^t E_{\text{cell}} I dt}{\Delta H m_{\text{added}}} \quad (21)$$

where ΔH is the heat of combustion (J mol⁻¹) and m_{added} is the amount (mol) of substrate added. This is usually calculated only for influents with known composition (i.e., for synthetic wastewaters) as ΔH is not known for actual wastewaters. In MFCs, energy efficiencies range from 2% to 50% or more when easily biodegradable substrates are used (18, 30). As a basis for comparison, the electric energy efficiency for thermal conversion of methane does not exceed 40%.

Distinguishing Methods of Electron Transfer

Presence of Mediators. Bacteria can reduce activation losses by increasing their extracellularly oriented mediation capacity. Three pathways are discerned at this point: direct membrane complex mediated electron transfer (8), mobile

redox shuttle mediated electron transfer (7), and electron transfer through conductive pili, also referred to as nanowires (9–11).

Cyclic voltammetry (CV) offers a rapid and proven method to discern whether bacteria use mobile redox shuttles to transfer their electrons, or pass the electrons “directly” through membrane associated compounds (6). For CV, a reference electrode is placed in the anode chamber of the MFC close to the anode (working electrode); the counter electrode (e.g., platinum wire) is preferably placed in the cathode chamber, but can also be placed in the anode chamber. A potentiostat is used to obtain a scan of potential. For bacterial suspensions, a scan rate of 25 mV s⁻¹ appears to be reasonable based on the work of several researchers (6, 73). For the analysis of mediators in biofilms, however, this scan rate needs to be decreased, possibly to 10 mV s⁻¹ and lower. This decrease can affect the accuracy of peak discrimination as the peaks tend to broaden.

The extent of the redox mediation and the midpoint potentials can be determined through analysis of (i) the MFC derived culture within its medium; (ii) the MFC culture after centrifugation and resuspension in physiological solution; and (iii) the supernatant of the centrifuged MFC culture. If a peak is found both in case (i) and (ii), it indicates a shuttle which is membrane associated. If a peak is found in case (i) and (iii), it indicates that a mobile, suspended shuttle is present. The size of the peaks, as integrated upon the voltammogram, either arbitrarily (as $\Sigma[\Delta I \Delta E \delta^{-1}]$) or through convolution analysis, does not correlate unequivocally to the extent of the membrane associated electron transfer and the mobile shuttle mediated electron transfer. This is caused by the restricted accessibility of the membrane associated shuttles for oxidation/reduction by the working electrode.

Presence of Nanowires. Electrically conductive bacterial appendages known as nanowires have only recently been discovered so their structure(s) are therefore not well studied or understood. Pili produced by some bacteria have so far been shown to be electrically conductive using scanning tunneling electron microscopy (11). There is no data at the present time whether nanowires can be detected or can be distinguished from adsorbed chemical shuttles via standard electrochemical methods such as CV. If electron shuttles associate with a nonconductive pili, or if the pili are covered with metal precipitates, they will be included in the CV measurements as membrane associated shuttles or may appear to be nanowires using STM. If redox shuttles are enclosed within the pilus’ tubular structure they are unlikely to be detected using CV. Additional research will be needed to determine the best methods for detecting nanowires and determining their importance relative to other methods of electron transfer from cells to electrodes.

Outlook

MFC designs need improvements before a marketable product will be possible (26, 74). Both the issues identified above and the scale-up of the process remain critical issues. Most of the designs reviewed here cannot be scaled to the level needed for a large wastewater treatment plant which requires hundreds of cubic meters of reactor volume. Either the intrinsic conversion rate of MFCs will need to be increased, or the design will need to be simplified so that a cost-effective, large-scale system can be developed. Designs that can most easily be manufactured in stacks, to produce increased voltages, will be useful as the voltage for a single cell is low.

The success of specific MFC applications in wastewater treatment will depend on the concentration and biodegradability of the organic matter in the influent, the wastewater temperature, and the absence of toxic chemicals. Materials costs will be a large factor in the total reactor costs. Mainly

anodic materials commonly used in MFC reactors, such as graphite foams, reticulated vitreous carbon, graphite, and others, are quite expensive. Simplified electrodes, such as carbon fibers, may alleviate these electrode costs. The use of expensive catalysts for the cathode must also be avoided. Another crucial aspect is the removal of non-carbon based substrates from the waste streams: nitrogen, sulfur, and phosphorus containing compounds often cannot be discharged into the environment at influent concentrations. Similarly, even particulate organic compounds will need to be removed and converted to easily biodegradable compounds, as part of an effective wastewater treatment operation.

Applications. One of the first applications could be the development of pilot-scale reactors at industrial locations where a high quality and reliable influent is available. Food processing wastewaters and digester effluents are good candidates. To examine the potential for electricity generation at such a site, consider a food processing plant producing 7500 kg/d of waste organics in an effluent (14). This represents a potential for 950 kW of power, or 330 kW assuming 30% efficiency. At an attained power of 1 kW/m³, a reactor of 350 m³ is needed, which would roughly cost 2.6 M Euros (26), at current prices. The produced energy, calculated on the basis of 0.1 Euros per kWh, is worth about 0.3 M Euros per year, providing a ten-year payback without other considerations of energy losses or gains compared to other (aerobic) technologies. Moreover, decreased sludge production could substantially decrease the payback time.

In the long term more dilute substrates, such as domestic sewage, could be treated with MFCs, decreasing society’s need to invest substantial amounts of energy in their treatment. A varied array of alternative applications could also emerge, ranging from biosensor development and sustained energy generation from the seafloor, to biobatteries operating on various biodegradable fuels.

While full-scale, highly effective MFCs are not yet within our grasp, the technology holds considerable promise, and major hurdles will undoubtedly be overcome by engineers and scientists. The growing pressure on our environment, and the call for renewable energy sources will further stimulate development of this technology, leading soon we hope to its successful implementation.

Acknowledgments

This research was supported by National Science Foundation (Grant BES-0401885 to B.L.), the Belgian Science Foundation (FWO grant G.0172.05 to W.V.), a Ph.D grant (IWT grant 41294 to P.A.) of the Institute for the Promotion of Innovation through Science and Technology in Flanders (IWT-Vlaanderen), Australian Research Council (DP 0666927 to J.K.), the Office of Naval Research (N00014-03-1-0431 to U.S.), and the German Research Foundation. Wetsus is funded by the city of Leeuwarden, the Province of Fryslân, the European Union European Regional Development Fund, and the EZ/KOMPAS program of the “Samenwerkingsverband Noord-Nederland”.

Literature Cited

- (1) Berk, R. S.; Canfield, J. H. Bioelectrochemical energy conversion. *Appl. Microbiol.* **1964**, *12*, 10–12.
- (2) Rao, J. R.; Richter, G. J.; Von Sturm, F.; Weidlich, E. The performance of glucose electrodes and the characteristics of different biofuel cell constructions. *Bioelectrochem. Bioenerg.* **1976**, *3*, 139–150.
- (3) Davis, J. B.; Yarbrough, H. F. Preliminary experiments on a microbial fuel cell. *Science* **1962**, *137*, 615–616.
- (4) Cohen, B. The bacterial culture as an electrical half-cell. *J. Bacteriol.* **1931**, *21*, 18–19.

- (5) Potter, M. C. Electrical effects accompanying the decomposition of organic compounds. *Proc. R. Soc. London Ser. B* **1911**, *84*, 260–276.
- (6) Rabaey, K.; Boon, N.; Siciliano, S. D.; Verhaege, M.; Verstraete, W. Biofuel cells select for microbial consortia that self-mediate electron transfer. *Appl. Environ. Microbiol.* **2004**, *70*, 5373–5382.
- (7) Rabaey, K.; Boon, N.; Hofte, M.; Verstraete, W. Microbial phenazine production enhances electron transfer in biofuel cells. *Environ. Sci. Technol.* **2005**, *39*, 3401–3408.
- (8) Bond, D. R.; Lovley, D. R. Electricity production by *Geobacter sulfurreducens* attached to electrodes. *Appl. Environ. Microbiol.* **2003**, *69*, 1548–1555.
- (9) Gorby, Y. A.; Beveridge, T. J. Composition, reactivity, and regulation of extracellular metal-reducing structures (nanowires) produced by dissimilatory metal reducing bacteria. Presented at DOE/NABIR meeting, April 20, 2005, Warrenton, VA.
- (10) Gorby, Y. A.; Yanina, S.; McLean, J. S.; Rosso, K. M.; Moyses, D.; Dohnalkova, A.; Beveridge, T. J.; Chang, I. S.; Kim, B. H.; Kim, K. S.; Culley, D. E.; Reed, S. B.; Romine, M. F.; Saffarini, D. A.; Hill, E. A.; Shi, L.; Elias, D. A.; Kennedy, D. W.; Pinchuk, G.; Watanabe, K.; Ishii, S.; Logan, B. E.; Nealson, K. H.; Fredrickson, J. K. Electrically conductive bacterial nanowires produced by *Shewanella oneidensis* strain MR-1 and other microorganisms. *PNAS* **2006**, in press.
- (11) Reguera, G.; McCarthy, K. D.; Mehta, T.; Nicoll, J. S.; Tuominen, M. T.; Lovley, D. R. Extracellular electron transfer via microbial nanowires. *Nature* **2005**, *435*, 1098–1101.
- (12) Bond, D. R.; Holmes, D. E.; Tender, L. M.; Lovley, D. R. Electrode-reducing microorganisms that harvest energy from marine sediments. *Science* **2002**, *295*, 483–485.
- (13) Park, D. H.; Zeikus, J. G. Utilization of electrically reduced neutral red by *Actinobacillus succinogenes*: physiological function of neutral red in membrane-driven fumarate reduction and energy conservation. *J. Bacteriol.* **1999**, *181*, 2403–2410.
- (14) Logan, B. E. Extracting hydrogen and electricity from renewable resources. *Environ. Sci. Technol.* **2004**, *38*, 160a–167a.
- (15) Kim, B. H.; Park, D. H.; Shin, P. K.; Chang, I. S.; Kim, H. J. Mediator-less biofuel cell. U.S. Patent 5976719, 1999.
- (16) Kim, H. J.; Park, H. S.; Hyun, M. S.; Chang, I. S.; Kim, M.; Kim, B. H. A mediator-less microbial fuel cell using a metal reducing bacterium, *Shewanella putrefaciens*. *Enzyme Microb. Technol.* **2002**, *30*, 145–152.
- (17) Min, B.; Logan, B. E. Continuous electricity generation from domestic wastewater and organic substrates in a flat plate microbial fuel cell. *Environ. Sci. Technol.* **2004**, *38*, 5809–5814.
- (18) Rabaey, K.; Lissens, G.; Siciliano, S. D.; Verstraete, W. A microbial fuel cell capable of converting glucose to electricity at high rate and efficiency. *Biotechnol. Lett.* **2003**, *25*, 1531–1535.
- (19) Rhoads, A.; Beyenal, H.; Lewandowski, Z. Microbial fuel cell using anaerobic respiration as an anodic reaction and biomineralized manganese as a cathodic reactant. *Environ. Sci. Technol.* **2005**, *39*, 4666–4671.
- (20) Shantaram, A.; Beyenal, H.; Raajan, R.; Veluchamy, A.; Lewandowski, Z. Wireless sensors powered by microbial fuel cells. *Environ. Sci. Technol.* **2005**, *39*, 5037–5042.
- (21) Barton, S. C.; Gallaway, J.; Atanassov, P. Enzymatic biofuel cells for implantable and microscale devices. *Chem. Rev.* **2004**, *104*, 4867–4886.
- (22) Ringeisen, B. R.; Henderson, E.; Wu, P. K.; Pietron, J.; Ray, R.; Little, B.; Biffinger, J. C.; Jones-Meehan, J. M. High power density from a miniature microbial fuel cell using *Shewanella oneidensis* DSP10. *Environ. Sci. Technol.* **2006**, *40*, 2629–2634.
- (23) Logan, B. E.; Murano, C.; Scott, K.; Gray, N. D.; Head, I. M. Electricity generation from cysteine in a microbial fuel cell. *Water Res.* **2005**, *39*, 942–952.
- (24) Phung, N. T.; Lee, J.; Kang, K. H.; Chang, I. S.; Gadd, G. M.; Kim, B. H. Analysis of microbial diversity in oligotrophic microbial fuel cells using 16S rDNA sequences. *FEMS Microbiol. Lett.* **2004**, *233*, 77–82.
- (25) Aelterman, P.; Rabaey, K.; Pham, T. H.; Boon, N.; Verstraete, W. Continuous electricity generation at high voltages and currents using stacked microbial fuel cells. *Environ. Sci. Technol.* **2006**, *40*, 3388–3394.
- (26) Rabaey, K.; Verstraete, W. Microbial fuel cells: novel biotechnology for energy generation. *Trends Biotechnol.* **2005**, *23*, 291–298.
- (27) Min, B.; Cheng, S.; Logan, B. E. Electricity generation using membrane and salt bridge microbial fuel cells. *Water Res.* **2005**, *39*, 1675–1686.
- (28) Oh, S.; Min, B.; Logan, B. E. Cathode performance as a factor in electricity generation in microbial fuel cells. *Environ. Sci. Technol.* **2004**, *38*, 4900–4904.
- (29) Oh, S.; Logan, B. E. Proton exchange membrane and electrode surface areas as factors that affect power generation in microbial fuel cells. *Appl. Microbiol. Biotechnol.* **2006**, *70*, 162–169.
- (30) Liu, H.; Logan, B. E. Electricity generation using an air-cathode single chamber microbial fuel cell in the presence and absence of a proton exchange membrane. *Environ. Sci. Technol.* **2004**, *38*, 4040–4046.
- (31) Park, D. H.; Zeikus, J. G. Improved fuel cell and electrode designs for producing electricity from microbial degradation. *Biotechnol. Bioeng.* **2003**, *81*, 348–355.
- (32) Cheng, S.; Liu, H.; Logan, B. E. Increased performance of single-chamber microbial fuel cells using an improved cathode structure. *Electrochem. Commun.* **2006**, *8*, 489–494.
- (33) Habermann, W.; Pommer, E. H. Biological fuel cells with sulphide storage capacity. *Appl. Microbiol. Biotechnol.* **1991**, *35*, 128–133.
- (34) Liu, H.; Ramnarayanan, R.; Logan, B. E. Production of electricity during wastewater treatment using a single chamber microbial fuel cell. *Environ. Sci. Technol.* **2004**, *38*, 2281–2285.
- (35) Rabaey, K.; Clauwaert, P.; Aelterman, P.; Verstraete, W. Tubular microbial fuel cells for efficient electricity generation. *Environ. Sci. Technol.* **2005**, *39*, 8077–8082.
- (36) He, Z.; Minter, S. D.; Angenent, L. T. Electricity generation from artificial wastewater using an upflow microbial fuel cell. *Environ. Sci. Technol.* **2005**, *39*, 5262–5267.
- (37) Reimers, C. E.; Tender, L. M.; Fertig, S.; Wang, W. Harvesting energy from the marine sediment–water interface. *Environ. Sci. Technol.* **2001**, *35*, 192–195.
- (38) Tender, L. M.; Reimers, C. E.; Stecher, H. A.; Holmes, D. E.; Bond, D. R.; Lowy, D. A.; Pilobello, K.; Fertig, S. J.; Lovley, D. R. Harnessing microbially generated power on the seafloor. *Nat. Biotechnol.* **2002**, *20*, 821–825.
- (39) Hasvold, Ø.; Henriksen, H.; Melvaer, E.; Citi, G.; Johansen, B. Ø.; Kjøningsen, T.; Galetti, R. Sea-water battery for subsea control systems. *J. Power Sources* **1997**, *65*, 253–261.
- (40) Heilmann, J. Microbial fuel cells: proteinaceous substrates and hydrogen production using domestic wastewater. Department Civil and Environmental Engineering, Penn State University, University Park, PA.
- (41) (a) Liu, H.; Grot, S.; Logan, B. E. Electrochemically assisted microbial production of hydrogen from acetate. *Environ. Sci. Technol.* **2005**, *39*, 4317–4320. (b) Logan, B. E.; Grof, S. A bioelectrochemically assisted microbial reactor (BEAMR) that generates hydrogen gas. Patent application 60/588, 022.
- (42) Rozendal, R. A.; Buisman, C. J. N. Process for producing hydrogen. Patent WO2005005981, 2005.
- (43) Rozendal, R. A.; Hamelers, H. V. M.; Euverink, G. J. W.; Metz, S. J.; Buisman, C. J. N. Principle and perspectives of hydrogen production through biocatalyzed electrolysis. *Int. J. Hydrogen Energy* **2006**, in press; DOI: 10.1016/j.ijhydene.2005.12.006.
- (44) Tanisho, S.; Kamiya, N.; Wakao, N. Microbial fuel cell using *Enterobacter aerogenes*. *Bioelectrochem. Bioenerg.* **1989**, *21*, 25–32.
- (45) Gil, G. C.; Chang, I. S.; Kim, B. H.; Kim, M.; Jang, J. K.; Park, H. S.; Kim, H. J. Operational parameters affecting the performance of a mediator-less microbial fuel cell. *Biosens. Bioelectron.* **2003**, *18*, 327–334.
- (46) Chaudhuri, S. K.; Lovley, D. R. Electricity generation by direct oxidation of glucose in mediatorless microbial fuel cells. *Nat. Biotechnol.* **2003**, *21*, 1229–1232.
- (47) Kim, N.; Choi, Y.; Jung, S.; Kim, S. Development of microbial fuel cell using *Proteus vulgaris*. *Bull. Korean Chem. Soc.* **2000**, *21*, 44–49.
- (48) Sell, D.; Krämer, P.; Kreysa, G. Use of an oxygen gas diffusion cathode and a three-dimensional packed bed anode in a bioelectrochemical fuel cell. *Appl. Microbiol. Biotechnol.* **1989**, *31*, 211–213.
- (49) Lowy, D. A.; Tender, L. M.; Zeikus, J. G.; Park, D. H.; Lovley, D. R. Harvesting energy from the marine sediment–water interface II – Kinetic activity of anode materials. *Biosens. Bioelectron.* **2006**, *21*, 2058–2063.
- (50) Niessen, J.; Schröder, U.; Rosenbaum, M.; Scholz, F. Fluorinated polyanilines as superior materials for electrocatalytic anodes in bacterial fuel cells. *Electrochem. Commun.* **2004**, *6*, 571–575.
- (51) Schröder, U.; Niessen, J.; Scholz, F. A generation of microbial fuel cells with current outputs boosted by more than one order of magnitude. *Angew. Chem., Int. Ed.* **2003**, *42*, 2880–2883.

- (52) Cheng, S.; Liu, H.; Logan, B. E. Increased power generation in a continuous flow MFC with advective flow through the porous anode and reduced electrode spacing. *Environ. Sci. Technol.* **2006**, *40*, 2426–2432.
- (53) Bergel, A.; Feron, D.; Mollica, A. Catalysis of oxygen reduction in PEM fuel cell by seawater biofilm. *Electrochem. Commun.* **2005**, *7*, 900–904.
- (54) Cheng, S.; Liu, H.; Logan, B. E. Power densities using different cathode catalysts (Pt and CoTMPP) and polymer binders (Nafion and PTFE) in single chamber microbial fuel cells. *Environ. Sci. Technol.* **2006**, *40*, 364–369.
- (55) Zhao, F.; Harnisch, F.; Schröder, U.; Scholz, F.; Bogdanoff, P.; Herrmann, I. Application of pyrolysed iron(II) phthalocyanine and CoTMPP based oxygen reduction catalysts as cathode materials in microbial fuel cells. *Electrochem. Commun.* **2005**, *7*, 1405–1410.
- (56) Rozendal, R. A.; Hamelers, H. V. M.; Buisman, C. J. N. Effects of membrane cation transport on pH and microbial fuel cell performance. *Environ. Sci. Technol.*, published online June 9, <http://dx.doi.org/10.1021/es060387r>.
- (57) Bard, A. J.; Parsons, R.; Jordan, J., Eds. *Standard Potentials in Aqueous Solution*; Marcel Dekker: New York, 1985.
- (58) Newman, J. S. *Electrochemical Systems*; Prentice Hall: Englewood Cliffs, NJ, 1973.
- (59) Alberty, R. A. *Thermodynamics of Biochemical Reactions*; John Wiley & Sons: New York, 2003.
- (60) Amend, J. P.; Shock, E. L. Energetics of overall metabolic reactions of thermophilic and hyperthermophilic Archaea and Bacteria. *FEMS Microbiol. Rev.* **2001**, *25*, 175–243.
- (61) Thauer, R. K.; Jungermann, K.; Decker, K. Energy conservation in chemotrophic anaerobic bacteria. *Bacteriol. Rev.* **1977**, *41*, 100–180.
- (62) Liu, H.; Cheng, S. A.; Logan, B. E. Production of electricity from acetate or butyrate using a single-chamber microbial fuel cell. *Environ. Sci. Technol.* **2005**, *39*, 658–662.
- (63) Hoogers, G., Ed. *Fuel Cell Technology Handbook*; CRC Press: Boca Raton, FL, 2003.
- (64) Larminie, J.; Dicks, A. *Fuel Cell Systems Explained*; John Wiley & Sons: Chichester, 2000.
- (65) Bard, A. J.; Faulkner, L. R. *Electrochemical Methods: Fundamentals and Applications*, 2nd ed.; John Wiley & Sons: New York, 2001.
- (66) He, Z.; Wagner, N.; Minteer, S. D.; Angenent, L. T. The upflow microbial fuel cell with an interior cathode: assessment of the internal resistance by impedance spectroscopy. *Environ. Sci. Technol.* **2006**, *40*, 5212–5217.
- (67) Park, D. H.; Laivenieks, M.; Guettler, M. V.; Jain, M. K.; Zeikus, J. G. Microbial utilization of electrically reduced neutral red as the sole electron donor for growth and metabolite production. *Appl. Environ. Microbiol.* **1999**, *65*, 2912–2917.
- (68) Bullen, R. A.; Arnot, T. C.; Lakeman, J. B.; Walsh, F. C. Biofuel cells and their development. *Biosens. Bioelectron.* **2006**, *21*, 2015–2045.
- (69) Heilmann, J.; Logan, B. E. Production of electricity from proteins using a single chamber microbial fuel cell. *Water Environ. Res.* **2006**, *78*, 531–537.
- (70) Niessen, J.; Schröder, U.; Scholz, F. Exploiting complex carbohydrates for microbial electricity generation – a bacterial fuel cell operating on starch. *Electrochem. Commun.* **2004**, *6*, 955–958.
- (71) Liu, H.; Cheng, S. A.; Logan, B. E. Power generation in fed-batch microbial fuel cells as a function of ionic strength, temperature, and reactor configuration. *Environ. Sci. Technol.* **2005**, *39*, 5488–5493.
- (72) Tchobanoglous, G.; Burton, F. L. *Wastewater Engineering: Treatment, Disposal and Reuse*, 3rd ed.; Metcalf & Eddy, McGraw-Hill: New York, 1991.
- (73) Park, H. S.; Kim, B. H.; Kim, H. S.; Kim, H. J.; Kim, G. T.; Kim, M.; Chang, I. S.; Park, Y. K.; Chang, H. I. A novel electrochemically active and Fe(III)-reducing bacterium phylogenetically related to *Clostridium butyricum* isolated from a microbial fuel cell. *Anaerobe* **2001**, *7*, 297–306.
- (74) Logan, B. E.; Regan, J. M. Microbial fuel cells – challenges and applications. *Environ. Sci. Technol.* **2006**, *40*, 5172–5180.
- (75) Rabaey, K.; Ossieur, W.; Verhaege, M.; Verstraete, W. Continuous microbial fuel cells convert carbohydrates to electricity. *Water Sci. Technol.* **2005**, *52*, 515–523.
- (76) Rosenbaum, M.; Schröder, U.; Scholz, F. In situ electrooxidation of photobiological hydrogen in a photobioelectrochemical fuel cell based on *Rhodobacter sphaeroides*. *Environ. Sci. Technol.* **2005**, *39*, 6328–6333.

Received for review March 2, 2006. Revised manuscript received May 22, 2006. Accepted June 7, 2006.

ES0605016